

# *The environmental setting of Epipalaeolithic aggregation site Kharaneh IV*

Article

Accepted Version

Jones, M. D., Maher, L. A., Macdonald, D. A., Ryan, C., Rambeau, C., Black, S. and Richter, T. (2016) The environmental setting of Epipalaeolithic aggregation site Kharaneh IV. *Quaternary International*, 396. pp. 95-104. ISSN 1040-6182 doi: <https://doi.org/10.1016/j.quaint.2015.08.092> Available at <http://centaur.reading.ac.uk/44811/>

It is advisable to refer to the publisher's version if you intend to cite from the work. See [Guidance on citing](#).

To link to this article DOI: <http://dx.doi.org/10.1016/j.quaint.2015.08.092>

Publisher: Elsevier

All outputs in CentAUR are protected by Intellectual Property Rights law, including copyright law. Copyright and IPR is retained by the creators or other copyright holders. Terms and conditions for use of this material are defined in

the [End User Agreement](#).

[www.reading.ac.uk/centaur](http://www.reading.ac.uk/centaur)

## **CentAUR**

Central Archive at the University of Reading

Reading's research outputs online

1  
2  
3  
4  
5  
6  
7  
8  
9  
10  
11  
12  
13  
14  
15  
16  
17  
18  
19  
20  
21  
22  
23  
24  
25  
26  
27  
28  
29  
30  
31  
32

**The environmental setting of Epipalaeolithic aggregation site Kharaneh IV**

Matthew D. Jones<sup>1\*</sup>, Lisa A. Maher<sup>2</sup>, Danielle A. Macdonald<sup>3,4</sup>, Conor Ryan<sup>5</sup>, Claire Rambeau<sup>6</sup>, Stuart Black<sup>7</sup>, and Tobias Richter<sup>8</sup>

1. School of Geography, University of Nottingham, University Park, Nottingham, NG7 2RD. UK
2. Department of Anthropology, University of California, Berkeley, USA
3. Department of Archaeological Science, University of Bradford, UK
4. Department of Anthropology, University of Tulsa, Harwell Hall, 800 S Tucker Drive, Tulsa OK, 74104
5. Golder Associates (UK) Ltd, Tadcaster, North Yorkshire, UK
6. Institut für Geo- und Umweltnaturwissenschaften – Geologie, University of Freiburg, Germany
7. Department of Archaeology, School of Archaeology, Geography and Environmental Science, University of Reading, UK
8. Department of Cross-Cultural and Regional, University of Copenhagen, Copenhagen, Denmark

\*Corresponding author: [matthew.jones@nottingham.ac.uk](mailto:matthew.jones@nottingham.ac.uk)

33 **Abstract**

34 The archaeological site of Kharaneh IV in Jordan's Azraq Basin, and its relatively near  
35 neighbour Jilat 6 show evidence of sustained occupation of substantial size through the Early  
36 to Middle Epipalaeolithic (c. 24,000 – 15,000 cal BP). Here we review the geomorphological  
37 evidence for the environmental setting in which Kharaneh IV was established. The on-site  
38 stratigraphy is clearly differentiated from surrounding sediments, marked visually as well as  
39 by higher magnetic susceptibility values. Dating and analysis of off-site sediments show that  
40 a significant wetland existed at the site prior to and during early site occupation (~ 23,000 –  
41 19,000 BP). This may explain why such a substantial site existed at this location. This  
42 wetland dating to the Last Glacial Maximum also provides important information on the  
43 palaeoenvironments and potential palaeoclimatic scenarios for today's eastern Jordanian  
44 desert, from where such evidence is scarce.

45

46

47 **Keywords:** Epipalaeolithic, Jordan, Last Glacial Maximum, Wetland, Azraq

## 48 **1. Introduction and Background**

49 There is much contemporary interest in people's relationships with their natural environment  
50 and how resources can be sustainably maintained given changing climates, population sizes,  
51 and per capita demands (e.g. Al-Juaidi et al., 2014; Berndtsson et al., 2014). Today people  
52 are increasingly vulnerable to risk associated with a changing climate and a finite resource  
53 base (e.g. IPCC, 2014). Arguably these issues were also critical for prehistoric societies,  
54 although for hunter-gatherers their ability to move around the landscape represented a  
55 highly flexible strategy through which climatic change could be effectively mitigated, as long  
56 as population levels remained relatively low. In the wider Levant region people's adaptation  
57 and mitigation strategies to a changing climate during the transition from the last glacial  
58 period into the Holocene interglacial have been widely discussed in relation to the  
59 beginnings of agriculture (e.g. Rosen, 2007; Blockley and Pinhasi, 2011; Maher et al.,  
60 2011a; Rosen and Rivera-Collazo, 2012). Yet our understanding of how the Levant  
61 experienced this global transition in climate is still somewhat unclear (e.g. Robinson et al.,  
62 2006; Enzel et al., 2008) and relies on palaeoclimatic datasets mainly from the west of the  
63 region. To improve our ability to test hypotheses about people's reactions to climatic and  
64 environmental change, or about their influence on climate and local environments (e.g.  
65 Ruddiman, 2015; Ramsey et al., in press), improved spatial and temporal resolution of our  
66 palaeoenvironmental and archaeological records is required (Maher et al., 2011a,).

67

68 The Azraq Basin of eastern Jordan has long been the focus of archaeological excavation and  
69 associated environmental investigations documenting a long history of human occupation  
70 dating back to the Lower Palaeolithic (e.g. Field, 1960; Copeland and Hours 1989; Rollefson  
71 et al., 1997; Betts, 1998; Garrard and Byrd, 2013). The latest set of excavations in the basin  
72 includes work by the Epipalaeolithic Foragers in Azraq Project (EFAP; e.g. Maher et al.,  
73 2011b, Maher et al. 2012; Richter et al., 2013; Maher et al., this volume) and this paper  
74 reports the results of geomorphological investigations around the site of Kharaneh IV, placing  
75 the site into its wider palaeoenvironmental context.

76

### 77 *1.1 Kharaneh IV*

78 The Early to Middle Epipalaeolithic site of Kharaneh IV (KHIV) is an important Late  
79 Pleistocene site in the Eastern Levant. Recent excavations at KHIV, building on the initial  
80 work of M. Muheisen (e.g. 1988), have shown the site to be of great archaeological interest.  
81 The high density of artefacts, given a relatively short occupation history (19,830-18,600 cal.  
82 years BP; Richter et al., 2013), as well as the thickness of archaeological deposits, large size  
83 of the site (22,000 m<sup>2</sup>), and the presence of very early hut structures (Maher et al., 2012; this

84 volume), are all rare for Epipalaeolithic sites and suggest frequent re-use of KHIV by hunter-  
85 gatherer groups.

86

87 The site is located approximately 40km west of the AzraqOasis (Fig. 1) at an elevation of  
88 ~640masl, lying on a sedimentary terrace of pale, cream-coloured silts, in the WadiKharaneh,  
89 just south of the Islamic castle of the same name. The local topography (Fig. 2) shows the  
90 site is the highpoint on the floor of the greater WadiKharaneh (Fig. 3); it sits at the confluence  
91 of two minor wadis with a general gradient of about 0.3m per 100m to the east, towards the  
92 central oasis.

93

94 The sediments around the site have been described very briefly before as part of regional  
95 reviews (Garrard et al., 1985; Besancon et al. 1989) but before EFAP were not dated or  
96 systematically surveyed to link KHIV into the wider landscape. Here we describe such work,  
97 providing a geomorphological background to the establishment of KHIV and adding to the  
98 palaeoenvironmental reconstruction of the local environment. In combination with faunal  
99 data (Martin et al, 2010, Jones, 2012) and ongoing archaeobotanical analysis, this  
100 geomorphological data contributes to our understanding of why this particular locality was  
101 selected for settlement and why people returned to the same place on the landscape for c.  
102 1000 years (see also Maher, in press). In addition, this work provides more information for  
103 an emerging picture of environmental change within the wider AzraqBasin through the late  
104 Quaternary (e.g. Jones and Richter, 2011; Cordova et al., 2013; Ames et al., 2014) that  
105 improves our understanding of regional environmental and climatic change throughout the  
106 Pleistocene and Holocene.

107

## 108 **2. Methodology**

### 109 *2.1 Mapping and sediment logging*

110 The topography of the site and the surrounding area was mapped in high-resolution using a  
111 ProMark3 differential GPS system, with survey data fixed to the local site grid. In total, 1076  
112 data points were used to create a local contour map of the site and the immediate  
113 surrounding area. Six off-site sections were dug into wadi terraces and were visually  
114 described and surveyed into the site grid. In addition, a 9m x 1m 'GeoTrench' was dug into  
115 the edge of the site itself. Careful surveying of all sections to the site grid allowed these off-  
116 site sections to be directly compared to the excavation areas on-site (see Maher et al., this  
117 volume for details of these). Of particular interest to this study are the deep sounding in  
118 Areas A (excavation square AS42) and B (R/S2/60) and a deep sounding between the  
119 two main excavation areas (AZ51), all of which were excavated into the archaeologically  
120 sterile units underlying the site.

121

## 122 2. 2 Age-estimates

123 A number of dating methods have been used to try and constrain the age of the stratigraphy,  
124 both on- and off-site, at KHIV. The methodologies for both Optically Stimulated  
125 Luminescence (OSL) and U-series approaches are outlined here.

126

127 OSL samples were taken in opaque tubes, sealed at both ends, from both off- and on-site  
128 sediments (detailed sampling locations are detailed later in the manuscript). On return from  
129 the field age estimates were obtained at the University of Gloucestershire Luminescence  
130 Dating Laboratory. All samples were opened and prepared under controlled laboratory  
131 illumination and to isolate material potentially exposed to daylight during sampling, sediment  
132 located within 20 mm of each tube-end was removed. The remaining sample was dried, and  
133 then subjected to acid and alkaline digestion to remove carbonate and organic components  
134 respectively. Fine silt sized quartz was extracted by sample sedimentation in acetone and  
135 feldspars and amorphous silica were then removed from this fraction through acid digestion  
136 (Jackson *et al.*, 1976; Berger *et al.*, 1980). Following addition of 10% HCl to remove acid  
137 soluble fluorides, grains degraded to  $<5 \mu\text{m}$  as a result of acid treatment were removed by  
138 acetone sedimentation. Up to 12 aliquots (ca. 1.5 mg) were then mounted on aluminium  
139 discs for Equivalent Dose ( $D_e$ ) evaluation.  $D_e$  values were quantified using a single-aliquot  
140 regenerative-dose (SAR) protocol (Murray and Wintle 2000; 2003) measuring the natural  
141 signal of a single aliquot and then regenerating that aliquot's signal by using known  
142 laboratory doses to enable calibration. For each aliquot, 5 different regenerative doses were  
143 administered so as to image dose response.  $D_e$  values for each aliquot were then  
144 interpolated, and associated counting and fitting errors calculated, by way of exponential  
145 plus linear regression. Weighted (geometric) mean  $D_e$  values were calculated, given  
146 sufficient mass, from 12 aliquots using the central age model outlined by Galbraith *et al.*  
147 (1999) and are quoted at  $1\sigma$  confidence (Table 1). Lithogenic Dose Rate ( $D_r$ ) values were  
148 defined through measurement of U, Th and K radionuclide concentration and conversion  
149 of these quantities into  $\alpha$ ,  $\beta$  and  $\gamma$   $D_r$  values (Table 1). Cosmogenic  $D_r$  values were calculated  
150 on the basis of sample depth, geographical position and matrix density (Prescott and Hutton,  
151 1994). Ages reported in Table 1 provide an estimate of sediment burial period based on  
152 mean  $D_e$  and  $D_r$  values and their associated analytical uncertainties.

153

154 A U-Series age was also obtained from carbonate nodules (e.g. Rowe & Maher 2000) found  
155 near the site (see sedimentary descriptions below for details). U/Th data was produced using  
156 a Perkin Elmer ELAN 6000 Inductively Coupled Plasma Mass Spectrometer at the University  
157 of Reading (e.g. Black *et al.* 2011; Rambeau *et al.* 2011). U/Th dating is based on the

158 measurement of  $^{230}\text{Th}$  produced by the radioactive decay of  $^{234}\text{U}$ , once the latter was  
159 preferentially incorporated into the newly precipitated sediment. The U/Th technique  
160 provides accurate dating only if 1) the system remains chemically closed after deposition,  
161 and 2) either if no initial Th is present within the system at time of precipitation, or the  
162 amount of additional Th (e.g., as brought in by detrital contamination) can be calculated and  
163 corrected for.

164

165 Collected samples were composed of dense, micritic carbonate and showed no sign of  
166 weathering internally, minimising the likelihood of dating problems due to open-system  
167 behaviour. As an attempt to correct for detrital contamination (that would add detrital thorium  
168 to the sediment dated, leading to calculation of ages that are too old) an isochron age was  
169 also calculated (e.g. Candy et al. 2004, 2005). Both individual and isochron ages were  
170 calculated using the program ISOPLOT© V.2.49 (Ludwig 2001), which also provides a  
171 statistical assessment of the validity of the calculated best-fit isochron age, by evaluating its  
172 relationship to the dataset (Mean Square of Weighted Deviates [MSWD], probability of fit).  
173 These statistics are crucial in estimating the accuracy of the calculated isochron age (Candy  
174 et al. 2004, 2005 and references therein); a high MSWD (value >1) indicates analytical or  
175 geological problems and ages that are potentially more complex..

176

### 177 *2.3 Sedimentology*

178 A series of standard sedimentary analyses were undertaken on a set of 52 samples to  
179 further quantify the visual sedimentary descriptions; 11 samples from Area A, 24 from Area  
180 B and 17 off-site samples (including those from the GeoTrench).

181

182 Loss on Ignition analysis was undertaken using standard procedures (e.g. Heiri et al., 2001).  
183 Volume-specific Magnetic Susceptibility analysis was undertaken using a Bartington MS2B  
184 Dual Frequency Magnetic Susceptibility Meter. Sub-samples were ground using a pestle and  
185 mortar, to achieve a homogeneous sample, and sieved at 0.25mm to remove any large  
186 clasts prior to analysis. X-ray Fluorescence (XRF) was undertaken on ground samples on  
187 a Panalytical Epsilon 3-XL at the School of Geography at the University of Nottingham with  
188 resulting spectra analysed to give values for the major oxides and elements MgO,  $\text{Al}_2\text{O}_3$ ,  
189  $\text{SiO}_2$ ,  $\text{K}_2\text{O}$ ,  $\text{CaO}$ ,  $\text{Ti}$ ,  $\text{Fe}_2\text{O}_3$  and Sr. Particle Size Analysis was undertaken using a Coulter LS  
190 200 Laser Granulometer after samples had been sieved at 1.4mm and disaggregated using  
191 a weak sodium hexametaphosphate solution. The GRADISTAT software package (Blott and  
192 Pye, 2001) was used to analyse this data.

193

## 194 **3. Results**



195  
196  
197  
198  
199  
200  
201  
202  
203  
204  
205  
206  
207  
208  
209  
210  
211  
212  
213  
214  
215  
216  
217  
218  
219  
220  
221  
222  
223  
224  
225  
226  
227  
228  
229  
230  
231

### 3.1 Sedimentology

The field descriptions of the five off-site sedimentary sections nearest to the site can be found below and their relative locations are shown in Figures 2 and 4. Section 3 was dug into the wadi south of the site and is not described here. In general, there are two major sedimentary units around the site 1) a series of pale coloured fine silts that make up the terrace on which the site sits, and 2) a series of reddish-brown, silts, sands and gravels (with clasts of flint) that are found in the wadi running to the south of the site.

#### *KHIV Section 1 (31 43' 27.1" N; 36 27'05.4" E)*

- 0 – 21 cm Light Red (10YR 7/6) silty sand with occasional roots. At base (16 – 21cm) large (2-5cm) flint clasts, some of which lie flat on the base of the unit.
- 21 – 26cm Pink (10YR 10/4) sand. Contains carbonate concretions and has secondary ?salt features suggesting soil formation during period of stasis or drying episode. Not laterally continuous over the site – predates an erosional episode prior to or during deposition of unit above.
- 26 – 30cm Same as the basal 5cm of top unit showing erosional features, rip up clasts into unit below and erosional surface on the upper contact.
- 30 – 62cm Light greenish grey (Gley 7/5GY) silty clay with very occasional large (>10cm) flint clasts. OSL sample GL11035 was taken from the top of this unit.

#### *KHIV Section 2 (31 43'27.8" N; 36 27'05.6"E)*

- 0 – 30cm Weathering surface and drape
- 30 – 73cm Pinkish white (10YR 8/2) homogenous silt. OSL sample GL11036 taken from 56cm depth.

#### *KHIV Section 4 (31 43' 22.5" N; 36 27' 13.0" E)*

- 0-12cm Very pale brown (10YR 7/4) silty fine sand containing small (1-3cm) clasts of flint and stone with roots to surface.
- 12-27cm Brownish yellow (10YR 6/6) fine sand with 2-5cm scale flint clasts. OSL sample GL11037 taken from this unit.
- 27-82 cm Light yellowish brown (10YR 6/4), but mottled, clayey silt with numerous fine roots and some larger roots.

232 *KHIV Section 5 (31 43'21.6" N; 36 27'21.0" E)*

233

234 0-10cm Weathering surface

235 10-92cm Very pale brown (10YR 8/2) silt with abundant root holes. OSL samples  
236 GL11038 and GL11039 taken from 40cm and 80cm respectively.

237 92-112cm Very pale brown (10YR 7/3) sandy silt with occasional small (1-2mm) flint  
238 specs.

239 112-137cm Very pale brown (10YR 7/4) silts with common small specs (1-2mm) of flint  
240 and charred plant remains or charcoal and occasional large (3-5cm) flints.

241

242 *KHIV Section 6 (31 43' 22.7" N; 36 27' 18.0" E)*

243

244 0-10cm Yellow (10YR 7/6) fine sand containing roots to the surface and plant  
245 remains. There is a dry crust on the Wadi surface.

246 10-36cm Light yellowish brown (10YR 6/4) sandy silt containing root holes and organic  
247 remains and occasional small (<1cm) flints. OSL sample GL11040 taken from the base of  
248 this section.

249 36 – 56cm Very pale brown (10YR 7/3) sand and gravel with large (>10cm) flint clasts.

250 56-111cm Yellowish brown (10YR 5/4) silty clay with occasional large flints.

251

252 *KHIV GeoTrench*

253 *Description based on Locus Summary Sheets*

254

255 0cm Locus 000 Surface

256 0-10cm Locus 001 Disturbed 10cm of slopewash on surface

257 10 – 25cm Locus 002 Red/brown Wadi Silt. OSL sample 11041 taken from this locus.

258 25 – 40cm Locus 003 Brown Clay – possible palaeosol in lake sediments?

259 40 – 43cm Locus 004 Upper White Clay

260 43 – 53cm Locus 005 Brown Clay. OSL sample GL11042 taken from this locus.

261 53 – 55cm Locus 006 Middle White Clay

262 55 – 70cm Locus 007 Brown 'Palaeosol'; looks like level of earliest site occupation given  
263 stratigraphy and comparison to sediments in AZ51.

264 70-72cm Locus 008 Lower White Clay looks like the white silt seen towards the base of  
265 AZ51 and in Sections 2 and 5

266

267 The sedimentological analyses (Table 1) show distinct differences between the on-site and  
268 off-site sediments particularly in terms of magnetic susceptibility and the amounts of calcium

269 and silica in the sediment. Average matrix grain size (Fig. 5) is slightly coarser on-site, most  
270 likely reflecting the anthropogenic origin of some of these sediments.

271

272 Given that there is little difference in iron content between the groups of samples it is likely  
273 that the substantial differences in magnetic susceptibility values reflect the amount of  
274 burning of the sediment onsite (e.g. Morinaga et al., 1999). Analysis of more samples would  
275 be required to confirm if the differences between Areas A and B are significant in terms of  
276 different intensities of burning throughout these areas, or if certain occupation layers have  
277 typically high magnetic susceptibility values. But these preliminary results do suggest this is  
278 an area of analysis that may warrant further investigation at the site.

279

280 The differences in elemental composition of the sediment, particularly in terms of calcium  
281 and silica reflect the visual description of these samples. CaO values from off-site samples  
282 are slightly skewed by the carbonate-rich silts of the terrace on which the site sits; samples  
283 in sections 1, 2 and 5 have an average of 42.2%. Sieving of these samples for other  
284 analyses, and during flotation on-site, reveals that they are rich in ostracod shells and we  
285 interpret them as carbonate-enriched wetland sediments, or marl.

286

### 287 *3.2 Age-estimates*

288 To provide an absolute chronology for the off-site sediments, where unlike in the site itself  
289 charcoal was not preserved, a series of OSL and U-Series age estimates were obtained  
290 (Tables 2 and 3). These, along with the radiocarbon chronology of the site, are  
291 summarised stratigraphically in Figure 4. Due to low amounts of material suitable for analysis  
292 in some OSL samples, some of these age estimates have to be treated with caution or as  
293 minimum ages. The lack of material in samples GL-11035, 11039, and 11041 restricted the  
294 number of aliquots available for  $D_e$  estimation. The latter 2 samples also did not have  
295 enough material to allow a dose recovery test, nor did samples 11046 and 11047. Sample  
296 GL11043 had significant feldspar contamination, such that this age is a minimum age  
297 estimate.

298

299 Analytically this leaves seven secure OSL age estimates. In the pale terrace silts we  
300 discount samples GL11044 and GL11045 based on stratigraphic reasons. These samples  
301 were taken from archaeologically sterile sediments directly below a well-constrained site age  
302 (Richter et al., 2013) and therefore cannot be younger than the site. The three other OSL  
303 age estimates, GL-11036, 11038 and 11042 give an age of 19 – 23 ka BP for the terrace  
304 silts. Although some caution is warranted in the use of this age range as the 'true' age of this  
305 unit, due to the clearly 'young' age estimates of samples GL11044 and GL11045, it is an age

306 that is supported by 4 of the age estimates from samples with limited datable material, and  
307 by the stratigraphic overlap of this unit with the site itself (19,830-18,600 cal. years BP;  
308 Richter et al., 2013).

309

310 From the second major sedimentary unit (the reddish browns silts, sands and gravels) two  
311 OSL age estimates (GL 11037 and 11040) place these deposits in the mid to late Holocene,  
312 5 – 3.5 ka BP. There are no analytically insecure age estimates from this unit, and  
313 stratigraphically they sit within the present day wadi, overlying the terrace silts in Section 1.

314

315 The individual U-Series ages on the carbonate nodules from the terrace surface gave an  
316 average age of  $22,740 \pm 920$  years. Individual ages were not corrected for detrital  
317 contamination, which  $^{230}\text{Th}/^{232}\text{Th}$  ratios show could be important (Table 3; low detrital  
318 contamination is usually indicated by high  $^{230}\text{Th}/^{232}\text{Th} > 25$ ; Candy et al. 2005). Although the  
319 uncorrected ages of all carbonate concretion subsamples seem highly coherent, an isochron  
320 age was calculated to try and take into account this contamination. However, the MSWD  
321 (120) and probability of fit (0), given by ISOPLOT as statistical assessment of the fit between  
322 the isochron and the original dataset, indicate a probable large degree of scatter around the  
323 best-fit isochron such that this age-estimate should be treated with great caution. Failure to  
324 obtain a statistically-meaningful isochron can be due to the fact that, although belonging to  
325 the same layer, the subsamples did not deposit at exactly the same time or contain different  
326 generations of carbonates (Candy et al. 2004); and/or there was more than one source of  
327 detrital contaminants. The subsamples also have very similar U-series ratios (Table 3),  
328 making it difficult to produce a well-defined isochron (e.g. Dean et al., 2015). This is  
329 exemplified by the degree of scatter shown on selected activity ratios (AR) plots (Fig. 6).  
330 Although the Rosholt plots,  $^{230}\text{Th}/^{232}\text{Th}$  AR versus  $^{238}\text{U}/^{232}\text{Th}$  (Rosholt I plot) and  $^{234}\text{U}/^{232}\text{Th}$   
331 AR versus  $^{238}\text{U}/^{232}\text{Th}$  (Rosholt II plot; Rosholt et al. 1976), emphasise alignment of  
332 subsamples, which suggests suitability for the construction of an isochron, the Osmond  
333 plots,  $^{230}\text{Th}/^{238}\text{U}$  AR versus  $^{232}\text{Th}/^{238}\text{U}$  (Osmond I plot) and  $^{234}\text{U}/^{238}\text{U}$  AR versus  $^{232}\text{Th}/^{238}\text{U}$   
334 (Osmond II plot; Osmond et al. 1970) highlight the clustering of subsamples due to chemical  
335 similarities which render them inappropriate for statistically meaningful isochron calculations.

336

337 The age of ca. 22,500-23,500 years given by both the individual dates and the isochron date  
338 should therefore be considered as a maximum age of the sample (since it cannot be  
339 properly corrected for initial detritalTh). This fits with the other chronological and stratigraphic  
340 controls on the site, as we presume these nodules formed during, or after the silts in which  
341 they sit (e.g. Rowe & Maher 2000) i.e. after c. 19 ka BP.

342

343 **4. Discussion**

344

345 The detailed mapping and absolute dating of the sediments surrounding KHIV allows us to  
346 reconstruct the environmental changes at the site for various time windows over the last  
347 23,000 years.

348

349 The spatial extent, duration and type of water body that deposited the pale terrace clays and  
350 silts at KHIV are difficult to establish. The present day extent of the marl terrace is clear from  
351 satellite imagery (Fig. 3) but as Garrard et al. (1985) noted there is no clear natural barrier to  
352 form a lake in this point on the wadi, and there are no shorelines evident against the  
353 limestone bedrock on the northern edge of the wadi. A more recent drainage pattern is now  
354 superimposed on the wadi, cutting the marl terrace between the site and section 5, and the  
355 main drainage channel of the WadiKharaneh to the north of the site may have eroded any  
356 remaining shoreline evidence.

357

358 The lack of distinct shoreline and other morphological features of the marl, such as the  
359 apparent parallel nature of the sedimentary units to the wadi floor, are similar to those  
360 defining ground-water discharge (GWD) deposits (Pigati et al., 2014). The sediments,  
361 especially those described in sections 2 and 5 often resemble those described as 'Wetland  
362 Marl' by Pigati et al. (2014) i.e. massive to blocky, which they interpretas forming in shallow  
363 wetlands, or in marshy areas. Of note at Kharaneh though is the massive nature of some of  
364 the marl, particularly in Section 2, suggesting there was little vegetation growing at the site of  
365 deposition. This suggests that the Kharanehwetland, at least at times, held substantial  
366 amounts of water and may have had open water areas.

367

368 Interpretation of this water body as being a GWD deposit is hard to envisage given the main  
369 Azraqaquifers today are at least 100m below Kharaneh (e.g. Al-Kharabsheh, 2000).

370 However, in times of more effective precipitation (see further discussion below) it is possible  
371 there was a localised, shallow, groundwater source at this location. Surface water recharge  
372 of this wetland may also have been possible. The marl terrace and the site sit in a  
373 particularly wide section of the main wadi channel, constrained by the limestone bedrock  
374 wadi edge to the north and the flint pavement (D in Figure 3) to the south. The full depth of  
375 the 'basin' in which the Pleistocene sediments of Kharaneh sit is unknown, but based on  
376 current topography this is a section of the wadi where flowing surface water could have  
377 slowed down and pooled, particularly in an area already rich in wetland vegetation. The  
378 recent digging of a dam near KHIV (clearly visible in Fig. 3) has shown that winter rains  
379 draining through WadiKharaneh today can last well into the summer months given sufficient

380 storage capacity. Given the spatial extent of the marl terrace it is likely that the Late  
381 Pleistocene wetland that produced these sediments would have been in the order of 50  
382 times larger than this dam, at least at its maximum extent.

383

384 The marl terrace, and therefore the wetland which deposited it, dates to between 23 and 19  
385 kaBP, based on the chronological discussion above. Today, there is a slight stratigraphic  
386 overlap between the top of sections 2 and 5, and the occupation levels of AZ51 on-site,  
387 given the regional topographic gradient (Figure 4). However, it is likely that this terrace was  
388 higher in the past. Besancon et al. (1989) describe carbonate concretions at the base of a  
389 30cm silt layer, we observe these nodules (from which the U-Series age estimates were  
390 produced) at or near the surface today, suggesting some substantial deflation in the ~30  
391 years between our surveys.

392

393 Under the western and northern areas of the site itself (Area A and AZ51), the  
394 wetland deposits are ostracod-rich, carbonate-concreted greenish marls, similar to those seen  
395 in sections 2 and 5, and are interstratified with the earliest Early EP occupations. Under the  
396 eastern portion of the site (Area B), archaeologically sterile, tan-coloured clays with little  
397 visible carbonate form an abrupt boundary (with no visible mixing) with the overlying  
398 occupational deposits (Maher et al., this volume). Given the subtle differences in the  
399 wetland facies observed on and around the site and their stratigraphic overlap with the site  
400 itself, and the microfossils observed during our initial analyses presented here (i.e. ostracods;  
401 diatoms are also preserved, K. Mills pers. com.) more detailed analysis of these  
402 wetland sediments are planned to tease out the detail of environmental change recorded  
403 here through the late Pleistocene.

404 Following the marl deposition Besancon et al. (1989) and Garrard et al. (1985) describe a  
405 silty loam (with carbonate concretions at the base) which today appears to have largely been  
406 deflated. Garrard et al. (1985) suggest these were loess deposits that, given our  
407 chronological data, were deposited at some point post-19 ka BP and would suggest  
408 substantial drying of the local environment. It's possible that these loess deposits are the  
409 same as those found in Locus 2 of the Geotrench (with a cautious age estimate of  $15 \pm 1$  ka  
410 BP; GL11041) but we are not able to link them together directly. The next depositional event  
411 related to the site is the Holocene fill identified in the minor wadis that make up the present  
412 day drainage pattern, dating to around 4 ka BP. This points to a substantial erosional phase  
413 of the marl terrace at some time between 19ka and 4ka BP.

414

415 *4.1 A suitable site for occupation?*

416 Given the location of the site, above much of the marl deposition, and also within the  
417 southern limits of the proposed maximum extent of the wetland(Fig. 3), it is unlikely that the  
418 most extensive Pleistocene water body still existed at Kharaneh at the time of the first site  
419 occupation around 20,000 years ago. However, as reported above, it seems likely that water  
420 did still exist at the site to some degree when it was first occupied, at least on a seasonal  
421 basis. Given the site's environmental history prior to occupation as documented  
422 here,Kharaneh IV would likely have appeared anoptimal location within a resource-rich  
423 environment in which to set up camp. The sustained occupation of the site suggests, despite  
424 limited sedimentary evidence post 19 ka BP, these resources were available for some time,  
425 at least 1200 years.

426

427 Jones and Richter (2011) show that the centralAzraq oasis was also a well-watered locale at  
428 this time and yet there is no large aggregation site apparent there. Archaeological evidence  
429 suggests that groups using different sets of lithic technology and with ties to either the west  
430 or the southern and northern Levant occupied the Azraq Basin during the Early  
431 Epipalaeolithic (Richter et al., 2011; Maher et al., this volume). It is possible that social  
432 barriers prevented the establishment of a large basecamp-style aggregation site in the oasis  
433 itself at that time. The AzraqOasis may have fallen in between territories of different social  
434 groups of hunter-gatherers making the establishment of a large site here socially  
435 unacceptable. This idea is supported by the fact that the only other large aggregation site in  
436 the Azraq Basin, Jilat 6, is characterised by a very different set of lithic industries compared  
437 to KHIV, whereas the lithic assemblages recovered from Ayn Qasiyya, a smaller site,have  
438 parallels with both the KHIV and Jilat 6 lithic assemblages. At the same time, it is also  
439 possible that the oasis may not have been suitable for long-term aggregated settlement due  
440 to other factors, such asthe presence of large predators. Given the long history of  
441 archaeological survey in and around the oasis it is unlikely that a site of the magnitude of  
442 Jilat 6 or KHIV has been missed.

443

444 Unfortunately there is no local sedimentary evidence from which to reconstruct the  
445 environment through most of the occupation of KHIV, or to point to reasons for eventual site  
446 abandonment. Such environmental information must come from ongoing work from the site  
447 itself. The now largely deflated loess deposits described by Garrard et al. (1985) and  
448 Besancon et al. (1989) does suggest a drier period following the wetlanddeposits that  
449 overlap with the site but there are nostratigraphically secure absolute dates to confirm if  
450 these were deposited during the site occupation, or following abandonment.

451

452 *4.2 Comparison to regional palaeoenvironmental records*

453 High lake levels during the Late Pleistocene are reported from across the wider eastern  
454 Mediterranean region, with water bodies substantially larger than those found today, such  
455 as Lake Lisan (e.g. Torfstein et al., 2013), Lake Van (Çağatay et al., 2014) and in the Konya  
456 plain (e.g. Roberts, 1983). A combination of increased precipitation and/or reduced  
457 evaporation is likely to have increased the potential (compared to present day conditions) for  
458 standing water to remain, where geomorphological conditions allowed. Both Lake Lisan and  
459 Konya had significant falls in lake levels ~ 21 ka BP and the deposits at Kharaneh IV would  
460 fit this pattern with the maximum extent of water at the site occurring before site occupation  
461 around 20 ka BP, and subsequent drying afterwards.

462

463 Evidence from other sites in the Azraq Basin would also suggest that the period of most  
464 positive water balance in the basin occurred shortly prior to 20 ka BP. Garrard et al. (1988,  
465 1994) and Garrard and Byrd (2013) interpret the sediments of Uweynid 14 (23.4 – 21.4 kcal  
466 BP; Richter et al., 2013) as being deposited during a period of relatively high water table and  
467 identify a 'humid' phase in the Wadi Jilat around 23 kcal BP (19,000 uncalibrated  
468 radiocarbon years BP). The timing of both these events would fit with the absolute dating of  
469 the Kharaneh marls. Organic marsh deposits are well established in the central oasis at Ayn  
470 Qasiyya by 24 ka BP as water levels fell from a more extensive open water body, although  
471 locally open water conditions there continued until 16 ka BP (Jones and Richter, 2011).

472

473 There is a lack of continuous post-Last Glacial Maximum sediments in the wider basin that  
474 make reconstructing environmental changes through the last glacial-interglacial transition  
475 and the early Holocene here difficult. For example in the central oasis there is a sedimentary  
476 hiatus at Ayn Qasiyya between 16 and 10.5 ka BP (Jones and Richter, 2011); we cannot  
477 therefore place events such as the net erosive period at KHIV between 19 and 4 ka BP  
478 with any better resolution. Identifying how environments in the Azraq Basin changed through  
479 this important transition remains a particular challenge of work in the region.

480

## 481 **5. Conclusions**

482

483 The Kharaneh wetland was likely a well-known landscape feature for Early  
484 Epipalaeolithic occupants of the Azraq Basin. As elsewhere in the region, a relatively positive  
485 hydroclimatic balance existed c. 23 ka BP. Water balance has not been as positive in the  
486 region since, having already begun to decline by the time of occupation at KHIV. With the  
487 central oasis providing persistent water and associated floral and faunal resources  
488 throughout this time period, KHIV and Jilat 6 additionally suggest the end of the Pleistocene  
489 was a prime time for people to thrive in the Azraq Basin, with a c. 1000 year window of rich



490 environmental resources that were substantially exploited by Early and Middle EP  
491 communities.

492

### 493 **Acknowledgements**

494 We thank the Department of Antiquities of Jordan and its Director General, our DoA reps for  
495 the field seasons at Kharanehand our DoA collaborator Ahmad Lash. We thank all the field  
496 crews of 2007-2015, in particular Samantha Allcock, and the community of Azraq for their  
497 continued support. This work was funded by grants from the Arts and Humanities Research  
498 Council of Britain, Council for British Research in the Levant, American Centre for Oriental  
499 Research, University of California, Berkeley, the Wenner-Gren Foundation, the University of  
500 Nottingham, and the Fragmented Heritage Project at the University of Bradford. Phil Toms is  
501 thanked for his advice on the interpretation of the OSL age estimates. This manuscript was  
502 written while MJ was a visiting Fellow in the School of Geography, Planning and  
503 Environmental Management at the University of Queensland. We thank Jason Rech and an  
504 anonymous reviewer for comments which improved this manuscript.

505 **References**

- 506 Al-Juaidi, A. E., Kaluarachchi, J. J., & Mousa, A. I. (2014). Hydrologic-Economic Model for  
507 Sustainable Water Resources Management in a Coastal Aquifer. *Journal of Hydrologic*  
508 *Engineering*, 19(11).
- 509 Al-Kharabsheh, A. (2000). Ground-water modelling and long-term management of the Azraq  
510 basin as an example of arid area conditions (Jordan). *Journal of arid environments*, 44(2),  
511 143-153.
- 512 Ames, Chris, April Nowell, Carlos Cordova, James Pokines and Michael Bisson. 2014. The  
513 Druze Marsh Paleolandscape: A Geoarchaeological Approach to Open-Air Paleolithic Sites.  
514 *Quaternary International* 331, 60-73.
- 515 Berger, G.W., Mulhern, P.J. and Huntley, D.J. (1980). Isolation of silt-sized quartz from  
516 sediments. *Ancient TL*, 11, 147-152.
- 517 Berndtsson, R., Jebari, S., Hashemi, H., & Wessels, J. (2014). Traditional water management  
518 techniques—do they have a role in post Arab Spring Middle East? *Hydrological Sciences*  
519 *Journal*.
- 520 Besançon, J., Geyer, B., Sanlaville, P., 1989. Contribution to the study of the geomorphology  
521 of the Azraq Basin, Jordan. In: Copeland, L., Hours, F. (Eds.), *The Hammer on the Rock:*  
522 *Studies in the Early Palaeolithic of Azraq*. British Archaeological Reports International Series  
523 540, Oxford, pp. 7-63.
- 524 Betts, A.V.G., 1998. *The Harra and the Hamad. Excavations and Surveys in Eastern Jordan*,  
525 Volume 1. Sheffield Academic Press, Sheffield.
- 526 Black S., Robinson S., Fitton R., Goodship R., and Rambeau C.M.C. 2011.  
527 Palaeoenvironmental and limnological reconstruction of Lake Lisan and the Dead Sea. In  
528 *Water Life and Civilisation: Climate, Environment and Society in the Jordan Valley*.  
529 International Hydrology Series. S. Mithen and E. Black (eds), Cambridge: Cambridge  
530 University Press
- 531 Blockley, S. P. E., & Pinhasi, R. (2011). A revised chronology for the adoption of agriculture in  
532 the Southern Levant and the role of Lateglacial climatic change. *Quaternary Science*  
533 *Reviews*, 30(1), 98-108.
- 534 Blott, S.J. and Pye, K. (2001) GRADISTAT: a grain size distribution and statistics package  
535 for the analysis of unconsolidated sediments. *Earth Surface Processes and Landforms* 26,  
536 1237-1248.
- 537 Çağatay, M. N., Öğretmen, N., Damcı, E., Stockhecke, M., Sancar, Ü., Eriş, K. K., & Özeren,  
538 S. (2014). Lake level and climate records of the last 90ka from the Northern Basin of Lake  
539 Van, eastern Turkey. *Quaternary Science Reviews*, 104, 97-116.
- 540 Candy, I., Black, S. and Sellwood, B.W. 2005. U-series Isochron Dating of Immature and  
541 Mature Calcretes as a Basis for Constructing Quaternary Landform Chronologies for the

542 Sorbas Basin, Southeast Spain. *Quaternary Research*, 64 pp. 100-111.

543 Candy, I., Black, S., Sellwood, B.W., 2004a. Quantifying timescales of pedogenic calcrete  
544 formation using U-series disequilibria. *Sedimentary Geology* 170, 177–187.

545 Copeland, L., and F. Hours. Editor. 1989. *The Hammer on the Rock: Studies in the Early*  
546 *Palaeolithic of Azraq, Jordan*. Oxford: B.A.R. International Series 540.

547 Cordova, Carlos, April Nowell, Michael Bisson, Christopher Ames, James Pokines, Melanie  
548 Chang and Maysoon al-Nahar. 2013. Glacial and Interglacial Desert Refugia and the Middle  
549 Paleolithic of the Azraq Basin, Jordan. *Quaternary International* 300, 194-210

550 Dean, J.R., Jones M.D., Leng, M.J., Noble, S.R., Metcalfe, S.E., Sloane H.J., Sahy, D.,  
551 Eastwood, W.J. and Roberts, C.N. 2015. Eastern Mediterranean hydroclimate over the late  
552 glacial and Holocene, reconstructed from the sediments of Nar Gölü, central Turkey, using  
553 stable isotopes and carbonate mineralogy. *Quaternary Science Reviews* 124, 290-295.

554 Enzel, Y., Amit, R., Dayan, U., Crouvi, O., Kahana, R., Ziv, B., & Sharon, D. (2008). The  
555 climatic and physiographic controls of the eastern Mediterranean over the late Pleistocene  
556 climates in the southern Levant and its neighboring deserts. *Global and Planetary*  
557 *Change*, 60(3), 165-192.

558 Field, H. 1960. *North Arabian Desert Archaeological Survey, 1925-1950. Papers of the*  
559 *Peabody Museum*. Cambridge: Peabody Museum, Harvard University.

560 Galbraith, R. F., Roberts, R. G., Laslett, G. M., Yoshida, H. and Olley, J. M. (1999) Optical  
561 dating of single and multiple grains of quartz from Jinmium rock shelter (northern Australia):  
562 Part I, Experimental design and statistical models. *Archaeometry*, 41, 339-364.

563 Garrard, A. N. and Byrd, B. 2013. *Beyond the Fertile Crescent: Late Palaeolithic and*  
564 *Neolithic communities of the Jordanian steppe. The Azraq Basin Project Volume 1: Project*  
565 *background and the Late Palaeolithic (geological context and technology)*. Oxford: Oxbow.

566 Garrard, A. N., 1998. Environment and cultural adaptations in the Azraq Basin: 24,000 -  
567 7,000 B.P. In: Henry, D.O., (Ed.) *The Prehistory of Jordan*. British Archaeological Reports  
568 International Series 705, Oxford, pp. 139-48

569 Garrard, A. N., Baird, D., Colledge, S., Martin, L., Wright, K., 1994. Prehistoric Environment  
570 and Settlement in the Azraq Basin: an interim report on the 1987 and 1988 Excavation  
571 Season. *Levant* 26, 73-109.

572 Garrard, A., Byrd, B., Harvey, P., & Hivernel, F. (1985). Prehistoric environment and  
573 settlement in the Azraq Basin. A report on the 1982 survey season. *Levant*, 17(1), 1-28.

574 Heiri, O., Lotter, A. F., & Lemcke, G. (2001). Loss on ignition as a method for estimating  
575 organic and carbonate content in sediments: reproducibility and comparability of  
576 results. *Journal of paleolimnology*, 25(1), 101-110.

577 IPCC, 2014: Summary for policymakers. In: *Climate Change 2014: Impacts, Adaptation, and*  
578 *Vulnerability. Part A: Global and Sectoral Aspects. Contribution of Working Group II to the*

579 Fifth Assessment Report of the Intergovernmental Panel on Climate Change [Field, C.B.,  
580 V.R. Barros, D.J. Dokken, K.J. Mach, M.D. Mastrandrea, T.E. Bilir, M. Chatterjee, K.L. Ebi,  
581 Y.O. Estrada, R.C. Genova, B. Girma, E.S. Kissel, A.N. Levy, S. MacCracken, P.R.  
582 Mastrandrea, and L.L. White (eds.)]. Cambridge University Press, Cambridge, United  
583 Kingdom and New York, NY, USA, pp. 1-32

584 Jackson, M.L., Sayin, M. and Clayton, R.N. (1976). Hexafluorosilicic acid regent modification  
585 for quartz isolation. *Soil Science Society of America Journal*, 40, 958-960.

586 Jones, J. R. (2012). Using gazelle dental cementum studies to explore seasonality and  
587 mobility patterns of the Early-Middle Epipalaeolithic Azraq Basin, Jordan. *Quaternary*  
588 *International*, 252, 195-201.

589 Jones, M. and T. Richter. 2011. Palaeoclimatic and archaeological implications of  
590 Pleistocene and Holocene environments in Azraq, Jordan. *Quaternary Research* Vol. 76 (3),  
591 363-372

592 Ludwig, K.R. 2001. ISOPLOT/Ex rev. 2.49, United States Geological Survey.

593 Maher L.A. Macdonald, D.A., Allentuck, A., Martin, L., Spyrou, A and Jones, M.D. *this*  
594 *volume* Occupying Wide Open Spaces? Late Pleistocene Hunter-Gatherer Activities in the  
595 Eastern Levant

596 Maher, L. (In review). Late Quaternary Refugia, Aggregations and Palaeoenvironments in  
597 the Azraq Basin. In *Quaternary Environments, Climate Change and Humans in the*  
598 *Levant*. Cambridge University Press: Cambridge.

599 Maher, L. A., Banning, E. B., & Chazan, M. (2011). Oasis or mirage? Assessing the role of  
600 abrupt climate change in the prehistory of the southern Levant. *Cambridge Archaeological*  
601 *Journal*, 21(1), 1-29.

602 Maher, L., Richter, T., Jones, M., Stock, J.T., 2011b. The Epipalaeolithic Foragers in Azraq  
603 Project: Prehistoric Landscape Change in the Azraq Basin, Eastern Jordan. CBRL Bulletin 6,  
604 21–27.

605 Maher, L.A., Richter, T., Macdonald, D., Jones, M.D., Martin, L., Stock, J.T., 2012. Twenty  
606 thousand-year-old huts at a hunter-gatherer settlement in eastern Jordan. PloS one 7,  
607 e31447.

608 Martin, L., Edwards, Y., & Garrard, A. (2010). Hunting practices at an eastern Jordanian  
609 Epipalaeolithic aggregation site: the case of Kharaneh IV. *Levant*, 42(2), 107-135.

610 Morinaga, H., Inokuchi, H., Yamashita, H., Ono, A., & Inada, T. (1999). Magnetic detection of  
611 heated soils at Paleolithic sites in Japan. *Geoarchaeology*, 14(5), 377-399.

612 Muheisen M (1988) The Epipalaeolithic phases of Kharaneh IV. In: Garrard A, Gebel H,  
613 editors. The Prehistory of Jordan The State of Research in 1986. Oxford: British  
614 Archaeological Reports 396. pp. 353-367.

615 Muheisen M (1988) The Epipalaeolithic phases of Kharaneh IV. In: Garrard A, Gebel H,  
616 editors. *The Prehistory of Jordan The State of Research in 1986*. Oxford: British  
617 Archaeological Reports 396. pp. 353-367.

618 Murray, A.S. and Wintle, A.G. (2000) Luminescence dating of quartz using an improved  
619 single-aliquot regenerative-dose protocol. *Radiation Measurements*, 32, 57-73.

620 Murray, A.S. and Wintle, A.G. (2003) The single aliquot regenerative dose protocol: potential  
621 for improvements in reliability. *Radiation Measurements*, 37, 377-381.

622 Osmond, J. K., J. P. May, and W. F. Tanner (1970), Age of the Cape Kennedy Barrier-and-  
623 Lagoon Complex, *Journal of Geophysical Research*, 75, 469–479.

624 Pigati, J.S., Rech, J.A., Quade, J. and Bright, J. (2014). Desert wetlands in the geologic  
625 record. *Earth-Science Reviews*, 132, 67-81.

626 Prescott, J.R. and Hutton, J.T. (1994) Cosmic ray contributions to dose rates for  
627 luminescence and ESR dating: large depths and long-term time variations. *Radiation*  
628 *Measurements*, 23, 497-500.

629 Rambeau C.M.C., Finlayson B., Smith S., Black S., Inglis R. and Robinson S. 2011.  
630 Palaeoenvironmental reconstruction at Beidha, southern Jordan (c. 18,000–8,500 BP):  
631 implications for human occupation during the Natufian and Pre-Pottery Neolithic. In *Water*  
632 *Life and Civilisation: Climate, Environment and Society in the Jordan Valley*. International  
633 Hydrology Series. S. Mithen and E. Black (eds), Cambridge: Cambridge University Press

634 Ramsey, M.N., Jones, M.D., Richter, T. and Rosen, A. *in press* Modifying the marsh:  
635 Evaluating Early Epipaleolithic hunter-gatherer impacts in the Azraq wetland, Jordan *The*  
636 *Holocene*

637 Richter, T, Garrard, A, Allcock, S & Maher, L 2011, 'Interaction Before Agriculture:  
638 Exchanging Material and Sharing Knowledge in the Final Pleistocene Levant' *Cambridge*  
639 *Archaeological Journal*, vol 21, no. 1, pp. 95-114.

640 Richter, T., Maher, L.A., Garrard, A.N., Edinborough, K., Jones, M.D., Stock, J.T., 2013.  
641 Epipalaeolithic settlement dynamics in southwest Asia: new radiocarbon evidence from the  
642 Azraq Basin. *Journal of Quaternary Science* 28, 467–479.

643 Roberts, N. (1983). Age, palaeoenvironments, and climatic significance of late Pleistocene  
644 Konya Lake, Turkey. *Quaternary Research*, 19(2), 154-171.

645 Robinson, S. A., Black, S., Sellwood, B. W., & Valdes, P. J. (2006). A review of  
646 palaeoclimates and palaeoenvironments in the Levant and Eastern Mediterranean from  
647 25,000 to 5000 years BP: setting the environmental background for the evolution of human  
648 civilisation. *Quaternary Science Reviews*, 25(13), 1517-1541.

649 Rollefson, G., Schnurrenberger, D., Quintero, L., Watson, R.P., Low, R., 1997. Ain Soda and  
650 'Ayn Qasiya: New late pleistocene and early Holocene sites in the Azraq Shishan area,

651 eastern Jordan. In: Gebel, H.G.K., Kafafi, Z., Rollefson, G.O. (Eds.) The prehistory of Jordan  
652 II. Perspectives from 1997. *ex oriente*, Berlin, 45-58.

653 Rosen, A. M. (2007). *Civilizing climate: social responses to climate change in the ancient*  
654 *Near East*. Rowman Altamira.

655 Rosen, Arlene M., and Isabel Rivera-Collazo 2012 Climate Change, Adaptive Cycles, and  
656 the Persistence of Foraging Economies during the Late Pleistocene/Holocene Transition in  
657 the Levant. *Proceedings of the National Academy of Sciences* 109(10): 3640–3645.

658 Rosholt, J.N. (1976) <sup>230</sup>Th/U dating of travertine and caliche rinds. The Geological Society of  
659 America, Abstracts and Program, 8: 1076 p.

660 Rowe P.J., Maher, B.A. (2000). 'Cold' stage formation of calcrete nodules in the Chinese  
661 Loess Plateau: evidence from U-series dating and stable isotope analysis.  
662 *Palaeogeography, Palaeoclimatology, Palaeoecology* 157, 109–125

663 Ruddiman, W. F., Ellis, E. C., Kaplan, J. O., & Fuller, D. Q. (2015). Defining the epoch we  
664 live in. *Science*, 348(6230), 38-39. Torfstein, A., Goldstein, S. L., Stein, M., & Enzel, Y.  
665 (2013). Impacts of abrupt climate changes in the Levant from Last Glacial Dead Sea  
666 levels. *Quaternary Science Reviews*, 69, 1-7.

667 **Figure and Table Captions**

668

669 **Figure 1** Extent of the Azraq basin (dashed line) showing major wadis (solid lines) and playa  
670 (hashed areas). The major archaeological sites discussed in the text are shown. Shading  
671 depicts 250m contour intervals (masl). The sites of Kharaneh IV and Ayn Qassiyya are also  
672 shown on the regional map for context.

673

674 **Figure 2** Detailed topography of the WadiKharaneh around the site of Kharaneh IV (here  
675 marked by the thick black line). The locations of the off-site sedimentary sections as  
676 described in the text are shown. The dotted line marks the transect described in Figure 4.

677

678 **Figure 3** Annotated satellite image of the site and surrounding area from Google Earth. The  
679 dotted line represents the maximum extent of the Kharaneh wetland, as defined by the  
680 bedrock topography and distribution of marl sediments.

681

682 **Figure 4**Relative distribution of off-site stratigraphy and occupational horizons of Kharaneh  
683 IV. All age estimates associated withthese sections are shown (bar one 'rejected' OSL date  
684 for the Geo Trench; GL11041); age estimates in bold are used in the final interpretations.  
685 The location of OSL samples are marked by circles (see Table 1 for details), the date of the  
686 present-day terrace surface was obtained using U-Series techniques (Table 2) and the date  
687 for the occupation horizons comes from Bayesian modelling of 13 radiocarbon age estimates  
688 (Richter et al., 2013). Note; for clarity the location of Section 4 has been moved, its actual  
689 location marked by the dotted outline. A full description of the sub-units of each section can  
690 be found in the main text.

691

692 **Figure 5**Particle size summaries for analysis of sediments taken from on- and off-site  
693 sections at KIV.

694

695 **Figure 6**Activity Ratio bi-plots from the U-Series analysis of carbonate nodules from near  
696 Kharaneh IV following Rosholt et al. (1976) and Osmond et al. (1970)

697

698 **Table 1**Data summary from sediment samples from Kharaneh IV and surrounding  
699 sediments. Mean values  $\pm$  1 standard deviation are shown.

700

701 **Table 2**Dose rate ( $D_r$ ), Equivalent Dose ( $D_e$ ) and Age data from Kharaneh IV OSL samples.  
702 Further discussion of the samples listed as having limited datable material or significant  
703 feldspar contamination can be found in the main text.

704

705 **Table 3** Uranium/Thorium age for sample KAL-IV. The isochron age is calculated using a  
706 series of subsamples (1-5). Uncorrected U/Th ages for each subsample are given in italics.  
707 Average uncertainties (SDs) on U and Th concentrations are calculated from all data  
708 measured during the same batch and are 0.45% and 0.67% respectively.

709

710



Figure 1

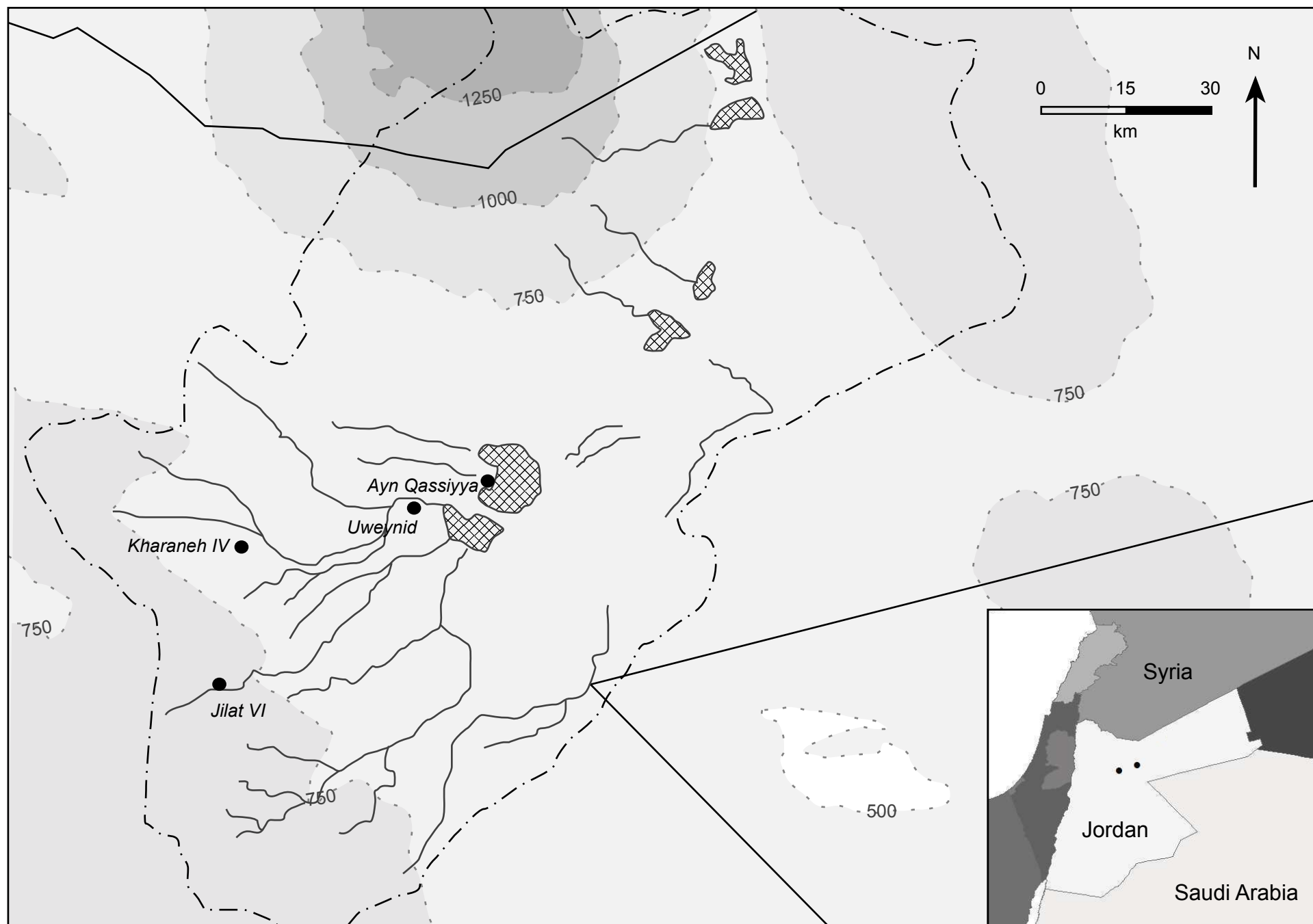


Figure 2

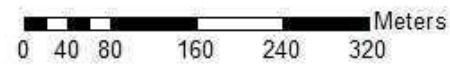
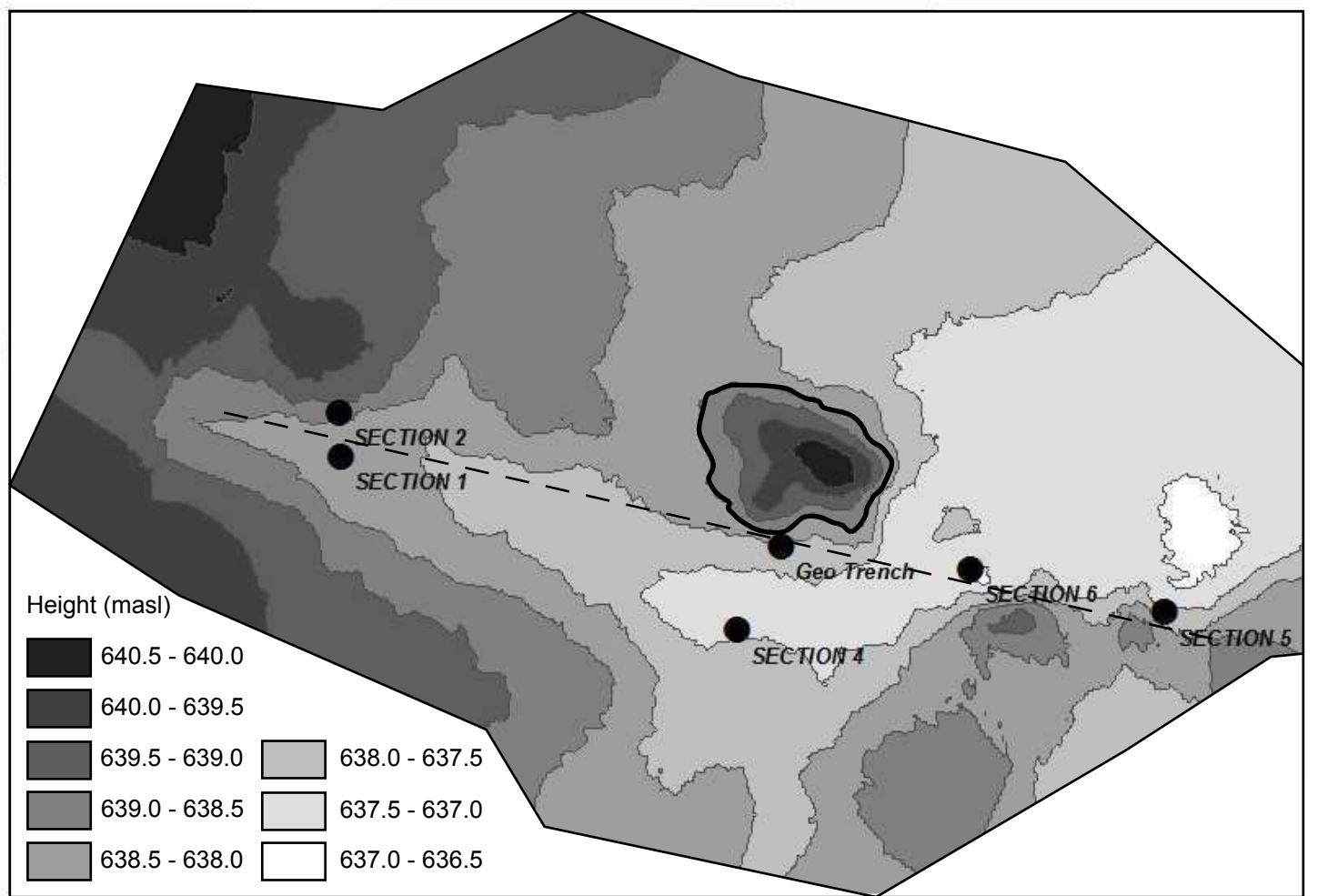


Figure 3

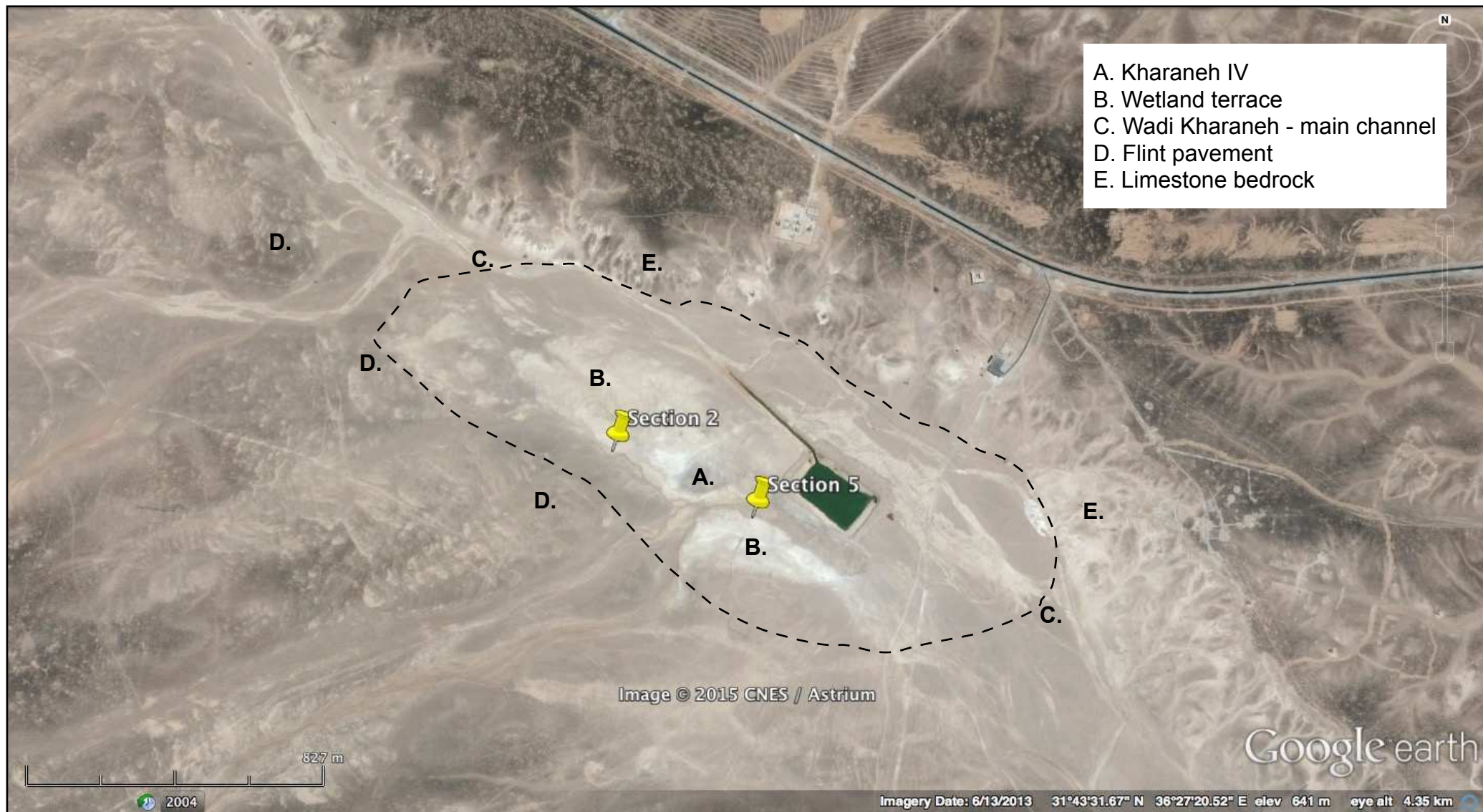


Figure 4

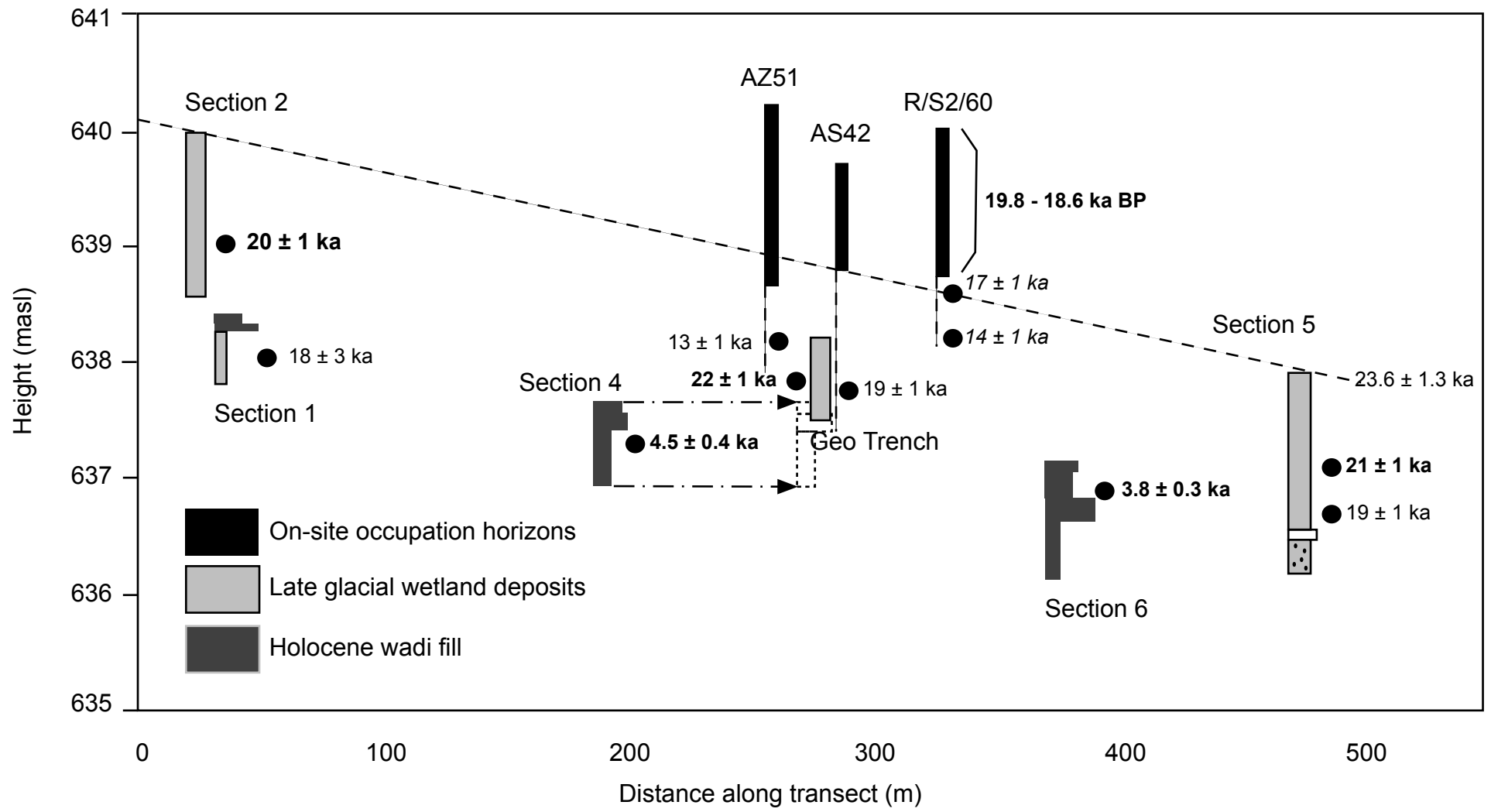


Figure 5

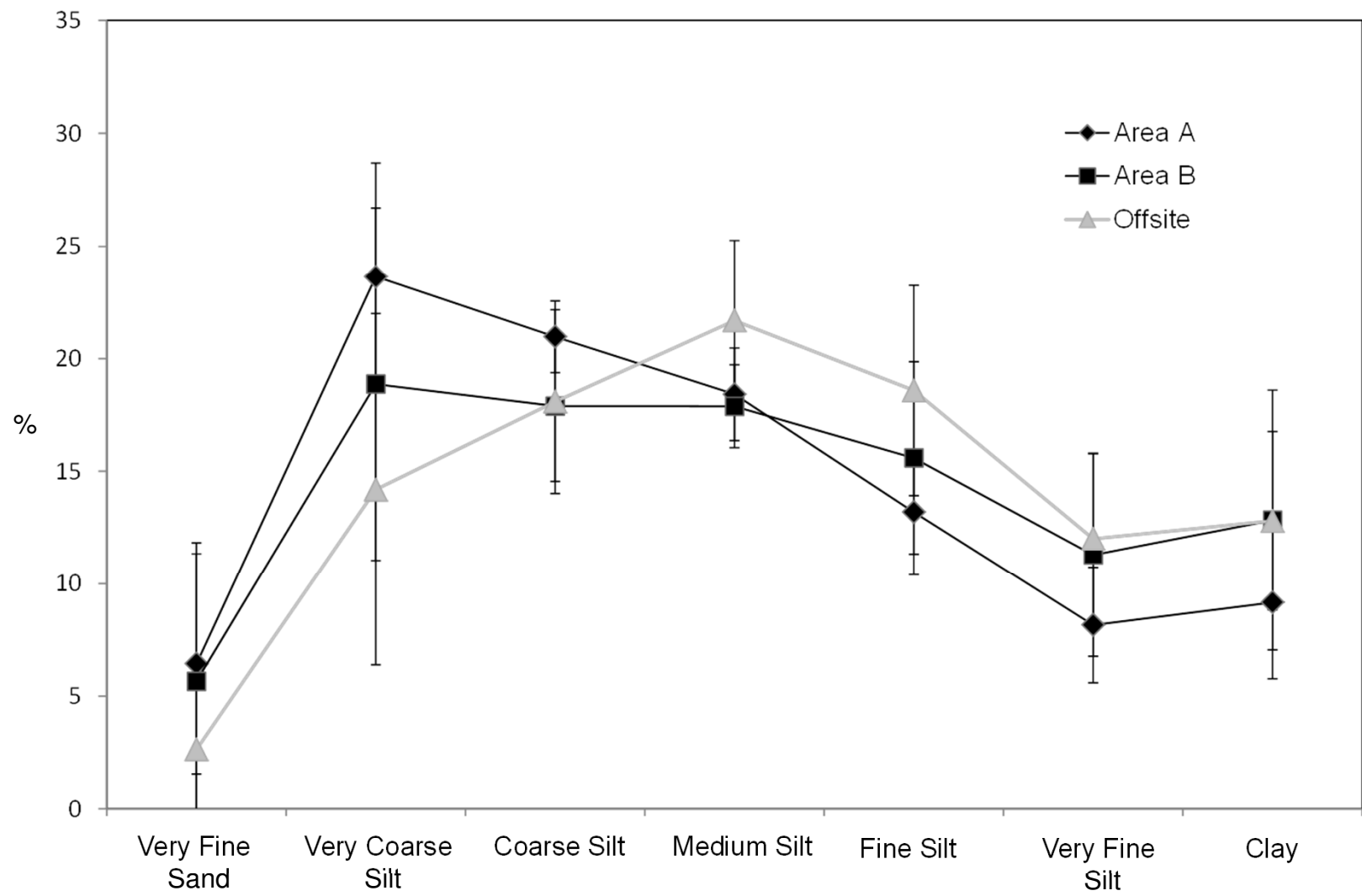
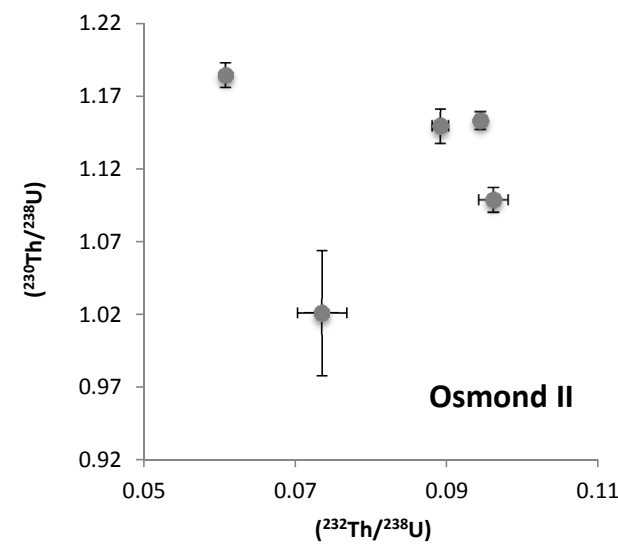
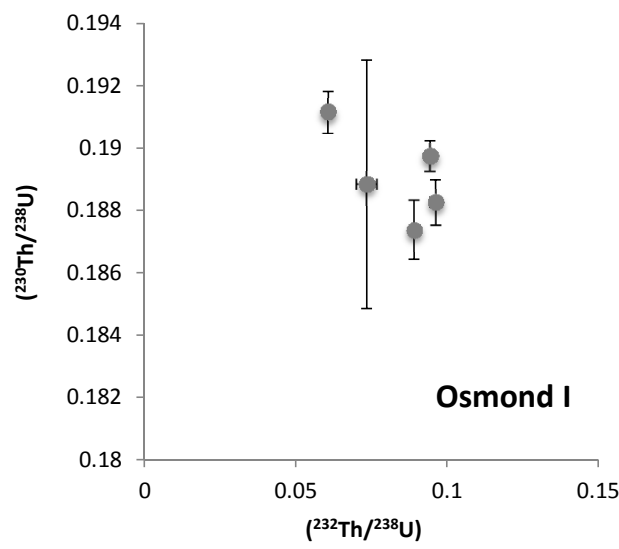
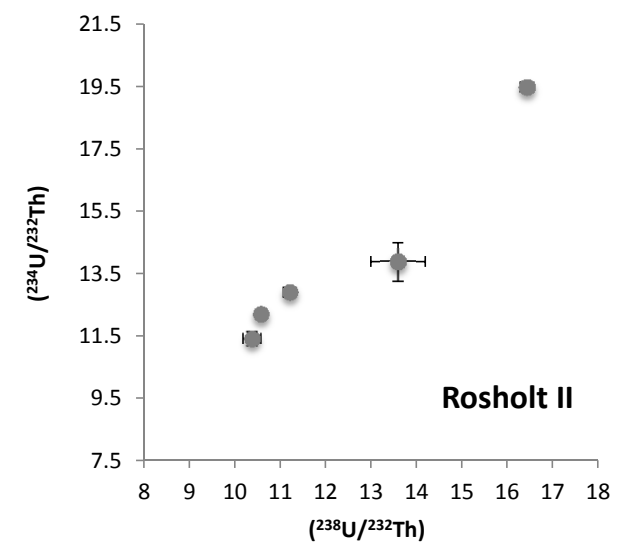
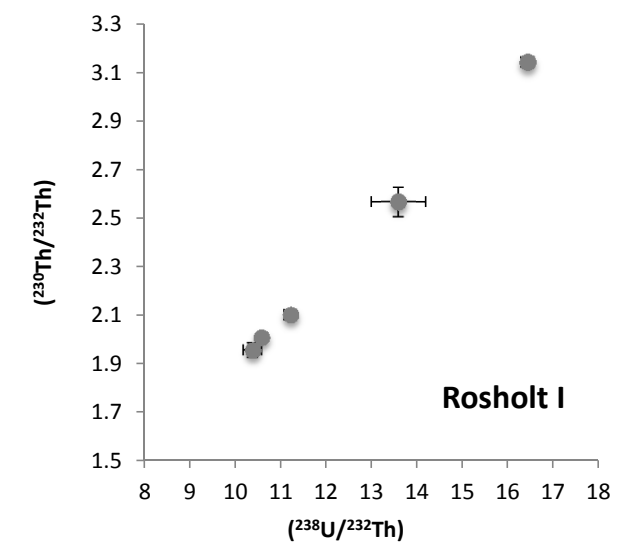


Figure 6



**Table 1** Data summary from sediment samples from Kharaneh IV and surrounding sediments. Mean values  $\pm$  1 standard deviation are shown.

| Samples locations  | Carbon content<br>% weight<br>loss at 550°C | Carbonate content<br>% weight<br>loss at 925°C | Magnetic<br>Susceptibility | MgO<br>%      | Al <sub>2</sub> O <sub>3</sub><br>% | SiO <sub>2</sub><br>% | K <sub>2</sub> O<br>% | CaO<br>%       | Ti<br>%       | Fe <sub>2</sub> O <sub>3</sub><br>% | Sr<br>%       |
|--------------------|---|--|----------------------------|---------------|-------------------------------------|-----------------------|-----------------------|----------------|---------------|-------------------------------------|---------------|
| Area A<br>(n=11)   | 9.0 $\pm$ 3.5                               | 10.7 $\pm$ 2.6                                 | 440.7 $\pm$ 100.8          | 6.2 $\pm$ 1.4 | 9.6 $\pm$ 1.0                       | 46.8 $\pm$ 3.4        | 1.2 $\pm$ 0.1         | 26.0 $\pm$ 3.7 | 0.7 $\pm$ 0.1 | 7.3 $\pm$ 1.0                       | 0.3 $\pm$ 0.1 |
| Area B<br>(n=24)   | 8.5 $\pm$ 2.3                               | 11.3 $\pm$ 2.8                                 | 224.4 $\pm$ 157.6          | 5.1 $\pm$ 0.7 | 10.7 $\pm$ 1.2                      | 46.0 $\pm$ 6.0        | 1.4 $\pm$ 0.3         | 26.2 $\pm$ 7.4 | 0.8 $\pm$ 0.1 | 9.2 $\pm$ 1.3                       | 0.2 $\pm$ 0.1 |
| Off-site<br>(n=17) | 7.8 $\pm$ 2.3                               | 13.7 $\pm$ 5.3                                 | 74.5 $\pm$ 15.9            | 3.8 $\pm$ 0.4 | 9.8 $\pm$ 1.5                       | 39.9 $\pm$ 5.5        | 1.0 $\pm$ 0.4         | 35.8 $\pm$ 8.3 | 0.7 $\pm$ 0.1 | 8.2 $\pm$ 1.1                       | 0.3 $\pm$ 0.2 |

Table 2

**Table 2** Dose rate ( $D_r$ ), Equivalent Dose ( $D_e$ ) and Age data from Kharaneh IV OSL samples. Further discussion of the samples listed as having limited datable material or significant feldspar contamination can be found in the main text.

| Field code     | Lab code | K %            | Th %           | U %            | $\alpha D_r$<br>Gy.ka <sup>-1</sup> | $\beta D_r$<br>Gy.ka <sup>-1</sup> | $\gamma D_r$<br>Gy.ka <sup>-1</sup> | Cosmic $D_r$<br>Gy.ka <sup>-1</sup> | Total $D_r$<br>Gy.ka <sup>-1</sup> | $D_e$<br>Gy  | Age<br>(ka)         | Comment                            |
|----------------|----------|----------------|----------------|----------------|-------------------------------------|------------------------------------|-------------------------------------|-------------------------------------|------------------------------------|--------------|---------------------|------------------------------------|
| Section 1      | GL11035  | 0.83<br>± 0.04 | 5.42<br>± 0.42 | 1.85<br>± 0.1  | 0.35<br>±0.02                       | 1.02<br>±0.05                      | 0.64<br>±0.03                       | 0.21<br>±0.02                       | 2.23<br>±0.07                      | 39.4<br>±7.2 | 18<br>± 3           | Limited datable material           |
| Section 2      | GL11036  | 1.07<br>± 0.05 | 6.22<br>± 0.44 | 2.02<br>± 0.11 | 0.39<br>±0.03                       | 1.25<br>±0.06                      | 0.76<br>±0.04                       | 0.19<br>±0.02                       | 2.59<br>±0.08                      | 51.4<br>±2.7 | <b>20</b><br>± 1    |                                    |
| Section 4      | GL11037  | 0.71<br>± 0.04 | 4.44<br>± 0.40 | 2.67<br>± 0.13 | 0.41<br>±0.03                       | 1.03<br>±0.05                      | 0.67<br>±0.03                       | 0.22<br>±0.03                       | 2.33<br>±0.07                      | 10.5<br>±0.8 | <b>4.5</b><br>± 0.4 |                                    |
| Section 5 40cm | GL11038  | 0.84<br>± 0.04 | 5.25<br>± 0.38 | 1.75<br>± 0.10 | 0.33<br>±0.02                       | 1.00<br>±0.05                      | 0.62<br>±0.03                       | 0.16<br>±0.02                       | 2.13<br>±0.07                      | 44.8<br>±2.7 | <b>21</b><br>± 1    |                                    |
| Section 5 80cm | GL11039  | 0.69<br>± 0.04 | 3.83<br>± 0.36 | 1.49<br>± 0.09 | 0.27<br>±0.02                       | 0.84<br>±0.04                      | 0.51<br>±0.03                       | 0.17<br>±0.02                       | 1.78<br>±0.06                      | 34.6<br>±2.3 | 19<br>± 1           | Limited datable material           |
| Section 6      | GL11040  | 0.97<br>± 0.05 | 6.76<br>± 0.52 | 2.23<br>± 0.11 | 0.42<br>±0.03                       | 1.21<br>±0.06                      | 0.77<br>±0.04                       | 0.22<br>±0.02                       | 2.62<br>±0.08                      | 10.0<br>±0.7 | <b>3.8</b><br>± 0.3 |                                    |
| Geo B OSL 1    | GL11041  | 0.96<br>± 0.05 | 6.06<br>± 0.44 | 2.10<br>± 0.11 | 0.38<br>± 0.03                      | 1.15<br>±0.06                      | 0.72<br>±0.04                       | 0.22<br>±0.02                       | 2.47<br>±0.08                      | 37.5<br>±1.5 | 15<br>± 1           | Limited datable material           |
| GEO B OSL 2    | GL11042  | 1.14<br>± 0.06 | 6.81<br>± 0.46 | 2.19<br>± 0.11 | 0.42<br>± 0.03                      | 1.33<br>±0.07                      | 0.81<br>±0.04                       | 0.21<br>±0.02                       | 2.77<br>±0.09                      | 61.1<br>±3.4 | <b>22</b><br>± 1    |                                    |
| AZ51 OSL       | GL11043  | 0.88<br>±0.05  | 5.79<br>± 0.43 | 1.97<br>± 0.10 | 0.37<br>±0.02                       | 1.08<br>±0.06                      | 0.68<br>±0.03                       | 0.18<br>±0.02                       | 2.32<br>±0.07                      | 30.6<br>±1.5 | 13<br>± 1           | Significant feldspar contamination |
| R/S2/60        | GL11044  | 1.12<br>± 0.05 | 6.46<br>± 0.45 | 1.91<br>± 0.10 | 0.38<br>±0.03                       | 1.27<br>±0.07                      | 0.76<br>±0.04                       | 0.18<br>±0.02                       | 2.59<br>±0.08                      | 36.6<br>±2.0 | <b>14</b><br>± 1    |                                    |
| R/S2/60        | GL11045  | 1.02<br>± 0.05 | 5.49<br>± 0.42 | 1.92<br>± 0.10 | 0.36<br>±0.02                       | 1.19<br>±0.06                      | 0.71<br>±0.03                       | 0.19<br>±0.02                       | 2.45<br>±0.08                      | 41.5<br>±2.2 | <b>17</b><br>± 1    |                                    |
| BS58 OSL 2     | GL11046  | 0.84<br>± 0.05 | 5.04<br>± 0.39 | 1.83<br>± 0.10 | 0.32<br>±0.02                       | 0.99<br>±0.06                      | 0.61<br>±0.03                       | 0.18<br>±0.02                       | 2.11<br>±0.07                      | 44.6<br>±2.1 | 21<br>± 1           | Limited datable material           |
| As42 OSL 4     | GL11047  | 0.67<br>0.04   | 4.24<br>± 0.4  | 2.07<br>± 0.11 | 0.34<br>±0.02                       | 0.90<br>±0.05                      | 0.57<br>±0.03                       | 0.17<br>±0.02                       | 1.99<br>±0.06                      | 38.4<br>±1.5 | 19<br>± 1           | Limited datable material           |



**Table 3** Uranium/Thorium age for sample KAL-IV. The isochron age is calculated using a series of subsamples (1-5). Uncorrected U/Th ages for each subsample are given in italics. Average uncertainties (SDs) on U and Th concentrations are calculated from all data measured during the same batch and are 0.45% and 0.67% respectively.

| <b>Sub-sample</b>              | <b>U<br/>(<math>\mu\text{g}/\text{kg}</math>)</b> | <b>Th<br/>(<math>\mu\text{g}/\text{kg}</math>)</b> | <b><math>^{234}\text{U}/^{238}\text{U}</math></b> | <b><math>^{230}\text{Th}/^{238}\text{U}</math></b> | <b><math>^{230}\text{Th}/^{232}\text{Th}</math></b> | <b>Age<br/>(y.BP)</b>                       |
|--------------------------------|---|--|---|--|---|---|
| KAL-IV-1                       | 8820  | 2412   | 1.150<br>$\pm 0.011$                              | 0.187<br>$\pm 0.001$                               | 2.100<br>$\pm 0.015$                                | <i>22509</i><br><i><math>\pm 910</math></i> |
| KAL-IV-2                       | 9832  | 2848   | 1.153<br>$\pm 0.006$                              | 0.190<br>$\pm 0.000$                               | 2.008<br>$\pm 0.007$                                | <i>22827</i><br><i><math>\pm 922</math></i> |
| KAL-IV-3                       | 12102   | 2256   | 1.185<br>$\pm 0.008$                              | 0.191<br>$\pm 0.001$                               | 3.144<br>$\pm 0.015$                                | <i>23016</i><br><i><math>\pm 930</math></i> |
| KAL-IV-4                       | 10018   | 2955   | 1.099 $\pm$<br>0.008                              | 0.188<br>$\pm 0.001$                               | 1.956<br>$\pm 0.030$                                | <i>22628</i><br><i><math>\pm 914</math></i> |
| KAL-IV-5                       | 7839  | 1768   | 1.021 $\pm$<br>0.043                              | 0.189<br>$\pm 0.004$                               | 2.567<br>$\pm 0.059$                                | <i>22705</i><br><i><math>\pm 918</math></i> |
| <b>Isochron Age (yrs B.P.)</b> |   |  |   |  |   | <b>23560 <math>\pm</math><br/>1247</b>      |